Rab1 Recruitment of p115 into a cis-SNARE Complex: Programming Budding COPII Vesicles for Fusion

Bernard B. Allan,* Bryan D. Moyer,* William E. Balch†

The guanosine triphosphatase Rab1 regulates the transport of newly synthesized proteins from the endoplasmic reticulum to the Golgi apparatus through interaction with effector molecules, but the molecular mechanisms by which this occurs are unknown. Here, the tethering factor p115 was shown to be a Rab1 effector that binds directly to activated Rab1. Rab1 recruited p115 to coat protein complex II (COPII) vesicles during budding from the endoplasmic reticulum, where it interacted with a select set of COPII vesicle–associated SNAREs (soluble *N*-ethylmaleimide–sensitive factor attachment protein receptors) to form a cis-SNARE complex that promotes targeting to the Golgi apparatus. We propose that Rab1-regulated assembly of functional effector-SNARE complexes defines a conserved molecular mechanism to coordinate recognition between subcellular compartments.

Vesicle traffic from the endoplasmic reticulum (ER) to the Golgi apparatus is controlled by the small guanosine triphosphatase (GTPase) Rab1 (*1, 2*). Rab1 is a member of the Ras superfamily of low molecular weight GTPases that cycle between inactive guanosine diphosphate (GDP)–bound and active GTP-bound forms (*3, 4*). To define the role of Rab1 in ER-to-Golgi transport, we set out to identify Rab1 effector molecules that specifically bind Rab1 in the GTP-bound form.

Incubation of rat liver cytosol with GST-Rab1-GTP [recombinant glutathione S-transferase (GST)–Rab1 fusion protein immobilized on glutathione-Sepharose beads and loaded with guanosine 5′-*O*-(3′-thiotriphosphate) (GTPγS)] preferentially retained a select set of putative effector proteins when compared to controls (Fig. 1A, asterisks) (*5*). Using immunoblotting (Fig. 1B), we found that p115, a factor that tethers membranes together before SNARE-regulated fusion (*6–8*), was a prominent protein retained by GST-Rab1-GTP beads (Fig. 1A, large asterisk). Retention of p115 on GST-Rab1-GTP beads was specific; *N*-ethylmaleimide–sensitive factor (NSF), sly1, β-COP, sec13, and other proteins involved in ER or Golgi function (*9, 10*) did not interact with GST-Rab1-GTP, nor did the early endosomal antigen 1 (EEA1) that binds Rab5-GTP (*11–13*) (Fig. 1B) (*14*).

p115 interacted with GST-Rab1-Q67L, a GTP-restricted mutant, but failed to interact with GST-Rab1-S25N, a GDP-restricted mutant, or GST-Rab1-N124I, a mutant that cannot stably bind guanine nucleotide (*1, 15, 16*) (Fig. 1C). Thus, activated Rab1 recognized p115. To examine whether this interaction was direct, we purified recombinant p115 after overexpression in insect cells (*17*). Purified p115 bound GST-Rab1-GTP beads, but not GST-Rab1-GDP beads (Fig. 1C). Furthermore, p115 did not interact with Rab2 or Sar1, other GTPases involved in ER-to-Golgi transport (*1, 18–20*), or with Rab3a, a GTPase involved in regulated secretory vesicle fusion (*21*) (Fig. 1D). Therefore, the tethering protein p115 was specifically and directly recognized by activated Rab1.

The yeast p115 homolog (Uso1p) is required for ER-to-Golgi transport (*8, 22*). Consistent with a potential role for p115 as a Rab1 effector protein, p115-specific monoclonal antibody (mAb), but not EEA1 mAb, inhibited an in vitro assay that reconstitutes transport of the cargo molecule vesicular stomatitis virus glycoprotein (VSV-G) between the ER and the Golgi apparatus in semi-intact cells (*23, 24*) (Fig. 2A). Immunodepletion of p115 from cytosol (*25*) partially inhibited transport, possibly reflecting a membrane-bound pool of p115. Inhibition was reversed by the addition of purified, recombinant p115 to levels found in cytosol (Fig. 2, B and C) (*26–28*). To identify the specific step in transport requiring p115, we used cell-free assays that separately reconstitute COPII vesicle budding and COPII vesicle fusion with Golgi membranes (*29, 30*). Although p115 mAb and p115-depleted cytosol had no effect on budding (*26*), both conditions inhibited fusion of COPII vesicles with Golgi membranes (Fig. 2D).

The primary function of a COPII vesicle is to transport newly synthesized cargo mol-

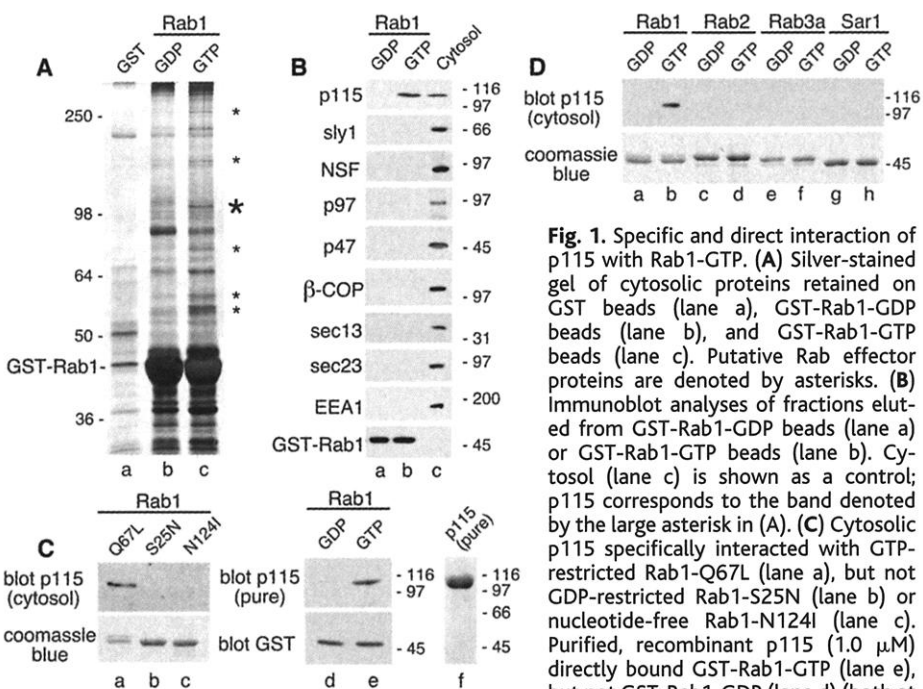

Fig. 1. Specific and direct interaction of p115 with Rab1-GTP. (**A**) Silver-stained gel of cytosolic proteins retained on GST beads (lane a), GST-Rab1-GDP beads (lane b), and GST-Rab1-GTP beads (lane c). Putative Rab effector proteins are denoted by asterisks. (**B**) Immunoblot analyses of fractions eluted from GST-Rab1-GDP beads (lane a) or GST-Rab1-GTP beads (lane b). Cytosol (lane c) is shown as a control; p115 corresponds to the band denoted by the large asterisk in (A). (**C**) Cytosolic p115 specifically interacted with GTP-restricted Rab1-Q67L (lane a), but not GDP-restricted Rab1-S25N (lane b) or nucleotide-free Rab1-N124I (lane c). Purified, recombinant p115 (1.0 μM) directly bound GST-Rab1-GTP (lane e), but not GST-Rab1-GDP (lane d) (both at 1.0 μM). Lane f shows Coomassie blue–stained gel of purified p115 (2 μg). (**D**) Cytosolic p115 specifically interacted with GST-Rab1 in the active, GTP-bound form (lanes a and b), but not with Rab2 (lanes c and d), Rab3a (lanes e and f), or Sar1 (lanes g and h). In (C) and (D), upper panels show immunoblots of bound p115; lower panels show Coomassie blue–stained gels or GST immunoblots illustrating GST-protein expression levels.

Departments of Cell and Molecular Biology, Scripps Research Institute, 10550 North Torrey Pines Road, La Jolla, CA 92037, USA.

*These authors contributed equally to this report.
†To whom correspondence should be addressed. E-mail: webalch@scripps.edu

ecules to the Golgi apparatus. Acquisition of vesicle-associated targeting and fusion machinery is likely to be linked to COPII vesicle formation. In this way, cargo delivery would be ensured by programming the vesicle for fusion during the budding step. One function of Rab GTPases may be to recruit effector molecules to membranes (*13, 31–33*). We performed experiments to determine whether Rab1 directs the binding of p115 to COPII vesicles during budding from the ER. For this purpose, we used Rab-GDI or Rab1-N124I, proteins that interfere with the normal Rab1 GTPase cycle and inhibit ER-to-Golgi transport (*1, 15, 34*). Rab-GDI extracts Rab proteins from membranes and prevents further Rab recruitment (*34, 35*); Rab1-N124I interferes with wild-type Rab function, possibly by preventing the exchange of GDP for GTP (*15, 36*).

p115 was recruited to budding COPII vesicles in a temperature-dependent manner (Fig. 3A). Moreover, a dominant negative mutant of Sar1, which is restricted to the GDP-bound form and blocks COPII vesicle budding (*29*), inhibited the appearance of p115 in the COPII vesicle fraction (Fig. 3A) and on affinity-purified COPII vesicles (Fig. 3B). Both Rab-GDI and Rab1-N124I inhibited recruitment of p115 onto budding COPII vesicles, but did not prevent COPII vesicle formation (Fig. 3A); thus, incorporation of p115 onto budding COPII vesicles was Rab1-dependent. When recruitment of p115 to newly formed COPII vesicles was blocked by inclusion of Rab1-N124I in the budding reaction (as in Fig. 3A), fusion with Golgi membranes was inhibited (Fig. 3C). Because cytosol in the fusion reaction, which contains p115, could not rescue vesicles formed in the presence of Rab1-N124I for fusion with Golgi membranes, inhibition of Rab1 function during the budding step is irreversible. We found that VSV-G cargo colocalized with p115, but not with EEA1, on COPII-derived membranes and pre-Golgi intermediates in transit to the Golgi apparatus in semi-intact cells (Fig. 3D) (*28*). Colocalization was evident when VSV-G was first visible in punctate ER export sites (Fig. 3D). Thus, Rab1-mediated recruitment of p115 onto COPII vesicles during budding programs vesicles for fusion with the Golgi apparatus.

The Rab1 and p115 homologs, Ypt1p and Uso1p, interact genetically with ER and Golgi SNARE proteins in yeast (*6, 37–41*). To identify potential physical interactions between p115 and SNAREs on COPII vesicles that may regulate docking and/or fusion with Golgi membranes, we cross-linked proteins on microsomal membranes before vesicle formation as well as on separated COPII vesicles that budded from these membranes (*30*). After solubilization, samples were immunoprecipitated with p115 mAb and immunoblotted for associated SNAREs and SNARE-binding proteins. Syntaxin5 (*42, 43*), sly1 [a syntaxin5 interacting protein (*44*)], membrin, and rbet1 were recovered in a cross-linked complex along with p115 (Fig. 4A, lane b) (*45*). Using quantitative immunoblotting (*45*), we found that negligible levels of SNAREs and SNARE-binding proteins were complexed with p115 on microsomal membranes, whereas 2 to 5% of COPII vesicle–associated SNAREs and SNARE-binding proteins were recovered in the p115 complex. This level, reflecting increased specific recovery of p115-SNARE complexes after formation of COPII vesicles, is similar to the reported recoveries of SNARE complexes directing other fusion events (*12, 46, 47*). Recovery of p115-SNARE complexes in the COPII vesicle fraction was dependent on budding, as incubations on ice or with Sar1-GDP prevented their appearance (Fig. 4A). These interactions were not detected in the presence of EEA1 mAb (Fig. 4A) or in the absence of cross-linker even when mild detergents were used to extract SNAREs from membranes (*26*), consistent with the inability to detect Uso1p-SNARE complexes in yeast cells (*6, 40*). Thus, previously reported interactions between Rab GTPases and SNAREs in yeast may be indirect and mediated by Rab effector proteins (*38, 48, 49*). Interaction of p115 with syntaxin5, sly1, and membrin was direct because purified, recombinant p115 and cytosolic p115, but not cytosolic EEA1, bound these proteins (Fig. 4B) (*50*). Neither purified nor cytosolic p115 bound the ER and Golgi SNARE rbet1, nor did they bind GST alone (Fig. 4B). Because immunoprecipitation of syntaxin5, membrin, or rbet1 from COPII vesicles led to reciprocal recovery of each of these SNAREs (*26*), association between p115 and rbet1 on COPII vesicles is likely to be through a specific physical interaction with the other SNAREs in the hetero-oligomeric cis-SNARE complex (Fig. 4A).

Although syntaxin5, sly1, membrin, and rbet1 were components of the p115 complex, we were unable to detect VSV-G, sec22, NSF, or Rab1 in the complex (Fig. 4A). Lack of Rab1 in the p115 complex is consistent with the proposed transient nature of Rab activation and Rab-effector interactions (*51*). Because Rab1 bound and recruited p115 to COPII vesicles during budding (Figs. 1 and 3) but was absent from the p115-SNARE complex, it is likely that the Rab1-p115 interaction precedes the p115-SNARE interaction.

To begin to investigate the function of the COPII vesicle–associated p115-SNARE complex in ER-to-Golgi transport, we performed vesicle budding reactions in the presence of SNARE antibodies to selectively deplete SNAREs from COPII vesicles. We previously used this strategy to demonstrate that syntaxin5 is required on COPII vesicles for fusion with Golgi membranes (*43*). Antibodies

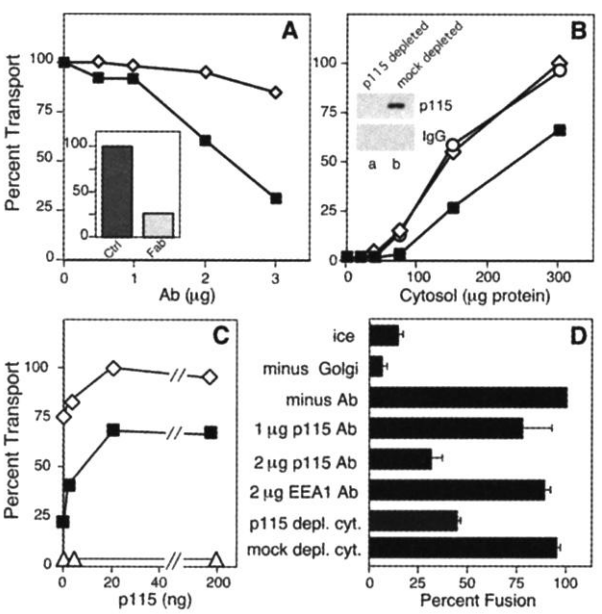

Fig. 2. p115 regulates ER-to-Golgi transport. (**A**) p115 mAb (solid squares), but not control EEA1 mAb (open diamonds), inhibited transport of VSV-G from the ER to the Golgi in semi-intact cells (*23, 24*). The amounts of VSV-G processed to the endoglycosidase H resistant form are reported relative to controls in which 50 to 60% of VSV-G was processed. Antibodies were preincubated in complete reaction mixtures for 30 min on ice before initiation of transport. p115 Fab fragments (12 μg) also blocked transport (inset). (**B**) p115-depleted cytosol (solid squares) inhibited transport in semi-intact cells compared to mock-depleted cytosol (using EEA1 mAb, open diamonds). Purified p115 (100 ng) restored transport to p115-depleted cytosol (open circles). Inset shows immunoblots of p115 levels (top) and absence of residual antibody (bottom) in p115-depleted (lane a) and mock-depleted (lane b) cytosols. (**C**) Dose-response curve showing effects of purified, recombinant p115 on VSV-G transport using p115-depleted cytosol (150 μg, solid squares), mock-depleted cytosol (150 μg, open diamonds), or no cytosol (open triangles) in semi-intact cells. (**D**) p115 mAb and p115-depleted cytosol inhibited fusion of COPII vesicles containing VSV-G with Golgi membranes. The amounts of VSV-G processed to the endo-D–sensitive form are reported relative to controls in which 40 to 45% of VSV-G was processed. Antibodies were preincubated for 15 min on ice in complete reaction mixtures before initiation of transport. Experiments were performed at least twice in (A), (B), and (C); results are depicted as mean ± SEM for at least four independent experiments in (D).

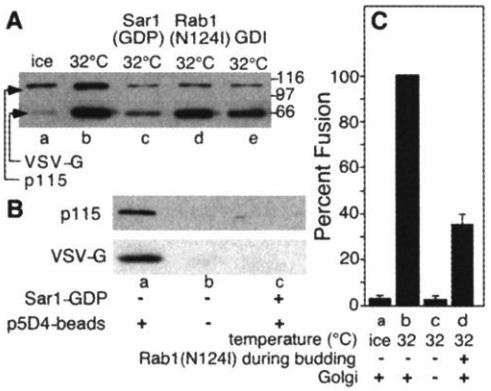

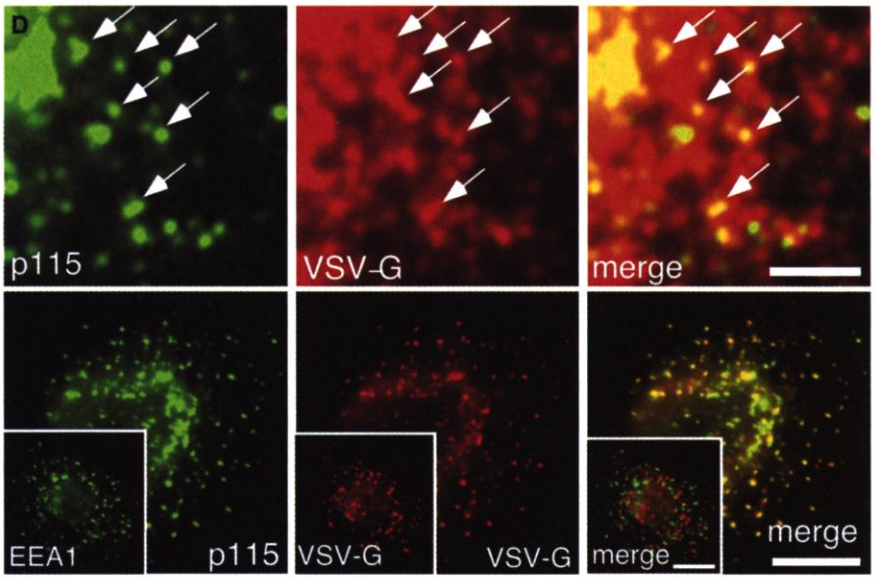

Fig. 3. Rab1 recruitment of p115 to budding COPII vesicles is necessary for fusion. (**A**) Rab1-N124I and Rab-GDI inhibited recruitment of p115 onto COPII vesicles. Immunoblots represent COPII vesicle fraction generated on ice (lane a) at 32°C for 10 min in the absence (lane b) or presence of Sar1-GDP (25 μg/ml, lane c), Rab1-N124I (20 μg/ml, lane d), or Rab-GDI (187.5 μg/ml, lane e). The reduced level of budding with Rab-GDI is consistent with our previous work (*34*). (**B**) p115 is present on purified COPII vesicles. COPII vesicle budding reactions were performed at 32°C for 10 min in the absence (lanes a and b) or presence (lane c) of Sar1-GDP (25 μg/ml). Vesicles were immunopurified using 10^7 M500 Dynabeads in the absence (lane b) or presence (lanes a and c) of VSV-G antibody p5D4 (*66*), as described (*29*). (**C**) Rab1-N124I inhibited fusion of vesicles with Golgi membranes when present in the budding reaction. Vesicles were generated in the presence or absence of Rab1-N124I as described in (A), and percent fusion with Golgi membranes was determined as in Fig. 2D. Results are depicted as mean ± SEM for three independent experiments. (**D**) p115, but not EEA1, colocalized with VSV-G cargo on COPII-derived transport intermediates. Digitonin-permeabilized cells were incubated with rat liver cytosol and ATP for 5 min (upper panels) or 45 min (lower panels) at 32°C (*67*). Cells were fixed and stained with the indicated antibodies. p115 is shown in green (left panels), VSV-G is shown in red (center panels), and merged images, in which colocalization is depicted in yellow, are shown in the right panels. (The insets, from left to right, show EEA1, VSV-G, and a merged image, using the same colors.) p115 also localized to Golgi membranes (*63*, *68*) that are dispersed in permeabilized cells (*67*). Scale bars, 1.5 μm for upper panels, 10 μm for lower panels.

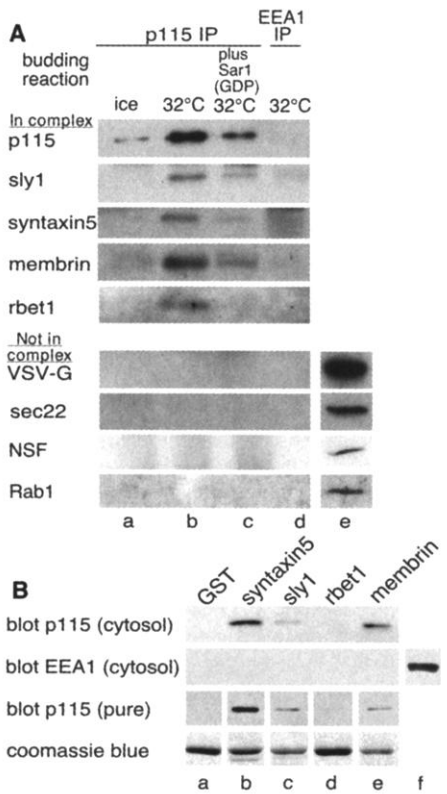

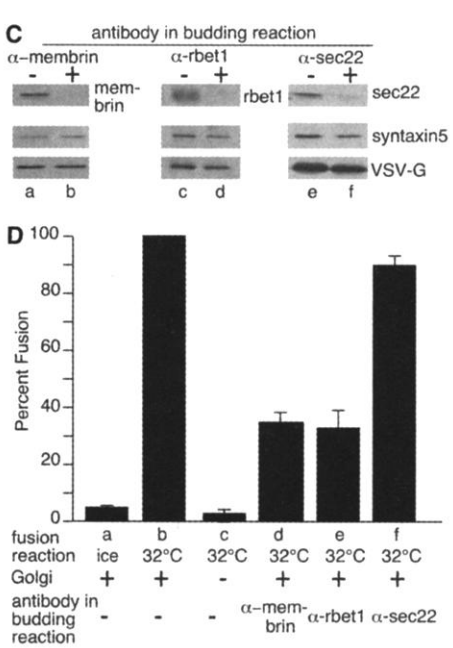

Fig. 4. Direct interaction of p115 with a select set of functional SNARE proteins in a macromolecular complex on COPII vesicles. (**A**) Cross-linking of p115 to SNARE proteins on COPII vesicles. COPII vesicle budding reactions were performed on ice (lane a) or at 32°C for 10 min in the absence (lanes b and d) or presence of Sar1-GDP (25 μg/ml, lane c). Vesicles were cross-linked with DTSSP (100 μM) and extracted in RIPA buffer, and p115 was immunoprecipitated with 2×10^7 M500 Dynabeads coupled to p115 mAb 3A10 (lanes a to c) or EEA1 mAb (lane d). Immunoprecipitates (lanes a to d) were immunoblotted for the indicated proteins. Recovery of p115 was 100%. Lane e shows membranes as control for antibodies recognizing proteins absent from the p115 complex. Results are representative of three independent experiments. (**B**) p115 directly interacted with ER and Golgi SNARE proteins. Cytosol (20 mg) or purified, recombinant p115 (0.5 μM) was incubated with GST alone (lane a), GST-syntaxin5 (lane b), GST-sly1 (lane c), GST-rbet1 (lane d), or GST-membrin (lane e) (all at 0.5 μM). Lane f shows cytosol as control for EEA1 mAb. Syntaxin5 beads retained 5 to 10 times the amount of p115 retained by sly1 or membrin beads. Results are representative of three independent experiments. (**C**) Antibodies to individual SNAREs specifically prevented the recruitment of these SNAREs to COPII vesicles. COPII vesicle budding reactions were performed at 32°C for 10 min in the presence or absence of the indicated antibodies (25 to 50 μg/ml). Vesicles were immunopurified using 10^7 M500 Dynabeads coupled to VSV-G antibody p5D4 (*66*). Proteins were separated by SDS-PAGE and immunoblotted for the indicated proteins. (**D**) Membrin and rbet1, but not sec22, are required on COPII vesicles for fusion with Golgi membranes. Vesicles were generated in the presence or absence of antibodies to SNARE's as in (C), and percent fusion with Golgi membranes was determined as in Fig. 2D. Results are depicted as means ± SEM for three independent experiments.

to membrin, rbet1, and sec22 selectively depleted COPII vesicles of these proteins without inhibiting budding or incorporation of syntaxin5 (Fig. 4C) or other SNAREs (*26*) to vesicles. Depletion of membrin or rbet1 from COPII vesicles inhibited fusion with Golgi membranes; however, depletion of sec22, which is not in the p115-SNARE complex and is not required for fusion in yeast (*37, 52–54*), did not affect fusion of COPII vesicles with the Golgi apparatus (Fig. 4D). Thus, the COPII vesicle–associated p115-SNARE complex displays functional specificity.

In summary, we have identified p115 as a direct downstream effector molecule of activated Rab1. Rab1 regulates ER-to-Golgi transport by recruiting p115 onto budding COPII vesicles where p115 interacts directly with a select set of SNARE proteins. In this manner, Rab1 directs COPII vesicles for delivery to Golgi membranes. These results may explain the Ypt1-dependent association of Uso1p on crude yeast membranes (*8*). Because Rab GTPases may also function late in fusion events (*55–58*), Rab1 recruitment of p115 may represent only the first step in a series of sequential protein-protein interactions between Rab1 and an assembling fusion complex. Additional putative Rab1 effector proteins (Fig. 1A) could fulfill the later functions for Rab1 in ER-to-Golgi transport (*15, 59*). Like Rab1, Rab5 has recently been shown to regulate the recruitment of a tethering factor (EEA1) into a macromolecular complex containing a syntaxin (syntaxin13) (*11–13*). Syntaxin13 is a SNARE required for homotypic endosome fusion in mammalian cells. A similar result has been observed for the EEA1 homolog (Vac1) in yeast (*60–62*). Our results suggest that Rab-mediated recruitment of tethering factors, such as p115 and EEA1, to membranes may be a general mechanism to coordinate vesicle formation with the assembly of microdomains containing macromolecular cis-SNARE complexes that program homotypic and heterotypic docking and fusion events.

References and Notes

1. E. J. Tisdale, J. R. Bourne, R. Khosravi-Far, C. J. Der, W. E. Balch, *J. Cell Biol.* **119**, 749 (1992).
2. H. Plutner *et al.*, *J. Cell Biol.* **115**, 31 (1991).
3. O. Martinez and B. Goud, *Biochim. Biophys. Acta* **1404**, 101 (1998).
4. F. Schimmoller, I. Simon, S. R. Pfeffer, *J. Biol. Chem.* **273**, 22161 (1998).
5. Bacterially expressed GST-Rab proteins (0.5 mg) were purified on glutathione-Sepharose beads (Pharmacia), loaded with GTPγS or GDP, incubated with gel-filtered rat liver cytosol (20 mg), and bound proteins eluted with EDTA as described (*11*) except that cells were lysed and washed in buffer containing 100 μM GTPγS instead of GDP during preparation of GST-Rab-GTP beads.
6. S. K. Sapperstein, V. V. Lupashin, H. D. Schmitt, M. G. Waters, *J. Cell Biol.* **132**, 755 (1996).
7. B. Sonnichsen *et al.*, *J. Cell Biol.* **140**, 1013 (1998).
8. X. Cao, N. Ballew, C. Barlowe, *EMBO J.* **17**, 2156 (1998).
9. M. Lowe and T. E. Kreis, *Biochim. Biophys. Acta* **1404**, 53 (1998).
10. R. Schekman and L. Orci, *Science* **271**, 1526 (1996).
11. S. Christoforidis, H. M. McBride, R. D. Burgoyne, M. Zerial, *Nature* **397**, 621 (1999).
12. H. M. McBride *et al.*, *Cell* **98**, 377 (1999).
13. A. Simonsen *et al.*, *Nature* **394**, 494 (1998).
14. The p115 mAbs used were 13F12 (specific for bovine p115; also known as mAb 115-5) and 3A10 (specific for rat p115) (*63, 64*). GST-Rab expression vectors and GST-SNARE expression vectors were generated using conventional techniques. EEA1 mAb was obtained from Transduction Laboratories (Lexington, KY). Antibodies to the cytoplasmic domains of membrin, rbet1, and sec22b were generated by injecting purified GST fusion proteins into the lymph nodes of female New Zealand white rabbits. Specific immunoglobulin G (IgG) antibodies were purified from serum by first passing a 36% ammonium sulfate cut over an Aminolink Plus (Pierce) GST column, to remove anti-GST IgGs, and then over a second Aminolink Plus column to which the specific antigen had been coupled. Antibodies were eluted in 1-ml fractions with 0.1 M glycine (pH 2.8) and 0.15 M NaCl directly into 0.1 ml of 1 M tris-HCl (pH 7.8).
15. S. Pind *et al.*, *J. Cell Biol.* **125**, 239 (1994).
16. C. N. Nuoffer, H. W. Davidson, J. Matteson, J. Meinkoth, W. E. Balch, *J. Cell Biol.* **125**, 225 (1994).
17. Bovine p115 cDNA was subcloned into the baculovirus expression vector pFastBac1, modified to contain a NH_2-terminal His_6 tag, to generate pFastBac1-p115. pFastBac1-p115 was transfected into Sf9 insect cells, and recombinant p115 baculovirus particles were isolated and amplified according to the manufacturer's instructions (Bac-to-Bac baculovirus expression system, Life Technologies). Tn5 insect cells (1 liter) were infected for 48 hours at 27°C with recombinant p115 baculovirus (~15 plaque-forming units per cell), pelleted at 3000 rpm for 20 min at 4°C, washed with 20 ml of ice-cold phosphate-buffered saline, repelleted as above, resuspended in 20 ml of lysis buffer [50 mM tris-HCl (pH 8.5), 100 mM KCl, 5 mM β-mercaptoethanol (β-ME), 1 mM phenylmethylsulfonyl fluoride, 1% NP-40, containing a Complete Protease Inhibitor Cocktail tablet (Roche Molecular Biochemicals)], snap-frozen in liquid N_2, and stored at −80°C. Lysates were thawed at 32°C and broken by nitrogen cavitation (500 psi, 30 min at 4°C). Lysates were then pelleted at 40,000 rpm for 60 min (Ti60 rotor) to remove insoluble material, and supernatants were incubated with 8 ml of 50% NTI-agarose slurry (Qiagen) pre-equilibrated with 10 column volumes of buffer A [20 mM tris-HCl (pH 8.5), 500 mM KCl, and 5 mM β-ME] for 45 min at 4°C with rotation. Beads were washed with 10 column volumes of buffer A and 10 columns of buffer B [20 mM tris-HCl (pH 8.5), 500 mM KCl, 10 mM imidazole, and 5 mM β-ME] and eluted in 1-ml aliquots with 3.5 column volumes of buffer C [20 mM tris-HCl (pH 8.5), 100 mM KCl, 100 mM imidazole, and 5 mM β-ME] at a flow rate of 1.0 ml/min. Fractions containing p115, determined by Coomassie blue staining and immunoblot analysis using p115 mAb 13F12, were pooled and dialyzed into NS buffer [25 mM Hepes (pH 7.4), 100 mM NaCl, 5 mM $MgCl_2$, and 1 mM dithiothreitol (DTT)] for binding assays or 25/125 [25 mM Hepes (pH adjusted to 7.4 with KOH) and 125 mM KOAc] for transport assays, snap-frozen in small aliquots in liquid N_2, and stored at −80°C. Purified p115 was >99% pure as determined by Coomassie blue staining. Before use, p115 protein was pelleted at 14,000 rpm for 10 min at 4°C to remove precipitated material.
18. E. J. Tisdale and W. E. Balch, *J. Biol. Chem.* **271**, 29372 (1996).
19. C. Barlowe *et al.*, *Cell* **77**, 895 (1994).
20. O. Kuge *et al.*, *J. Cell Biol.* **125**, 51 (1993).
21. G. Fischer von Mollard, B. Stahl, C. Li, T. C. Sudhof, R. Jahn, *Trends Biochem. Sci* **19**, 164 (1994).
22. C. Barlowe, *J. Cell Biol.* **139**, 1097 (1997).
23. C. J. M. Beckers, D. S. Keller, W. E. Balch, *Cell* **50**, 523 (1987).
24. H. W. Davidson and W. E. Balch, *J. Biol. Chem.* **268**, 4216 (1993).
25. Rat liver cytosol (2 mg) was incubated with p115 mAb 3A10 (2 μg) or mock EEA1 antibody in 1 ml of NS buffer containing 0.1% β-octylglucoside at 4°C overnight with rotation. Detergent was required to quantitatively immunoprecipitate p115. p115-antibody complexes were precipitated with 25 μl of protein G–Sepharose 4 Fast Flow (Amersham), preblocked with 1% bovine serum albumin (BSA), for 2 hours at 4°C with rotation. Immune complexes were pelleted at 14,000 rpm for 30 s and the supernatant, containing p115-depleted cytosol, was removed, concentrated to 25 to 30 mg/ml using Nanosep microconcentrators (molecular weight cutoff 10,000; Pall Filtron Corp., Northborough, MA), and microdialyzed overnight into 25/125 (*17*) to remove detergent. Cytosol was snap-frozen in small aliquots in liquid N_2 and stored at −80°C. Immunoblot analysis using p115 mAb 3A10 confirmed quantitative removal (>99%) of p115 from cytosol.
26. B. B. Allan, B. D. Moyer, W. E. Balch, unpublished data.
27. J. Shorter and G. Warren, *J. Cell Biol.* **146**, 57 (1999).
28. C. Alvarez, H. Fujita, A. Hubbard, E. Sztul, *J. Cell Biol.* **147**, 1205 (1999).
29. T. Rowe *et al.*, *J. Cell Biol.* **135**, 895 (1996).
30. To measure COPII vesicle budding, we incubated ER microsomes containing VSV-G with cytosol and adenosine triphosphate (ATP) at 32°C. The released COPII vesicles were separated from ER microsomes by differential centrifugation and collected by high-speed centrifugation. The appearance of VSV-G in the high-speed pellet (HSP) is a direct measure of COPII vesicle budding from the ER (*29*). For measurement of fusion, COPII vesicles recovered in the HSP were incubated with purified Golgi membranes in a separate reaction and fusion was measured by processing of VSV-G to the endoglycosidase D (endo D)–sensitive form, a hallmark of transport to the cis-Golgi network (*23, 29*).
31. H. Stenmark, G. Vitale, O. Ullrich, M. Zerial, *Cell* **83**, 423 (1995).
32. G. Vitale *et al.*, *EMBO J.* **17**, 1941 (1998).
33. B. Stahl, J. H. Chou, C. Li, T. C. Sudhof, R. Jahn, *EMBO J.* **15**, 1799 (1996).
34. F. Peter, C. Nuoffer, S. N. Pind, W. E. Balch, *J. Cell Biol.* **126**, 1393 (1994).
35. S.-K. Wu *et al.*, *J. Biol. Chem.* **273**, 26931 (1998).
36. L. A. Feig, *Nature Cell Biol.* **1**, E25 (1999).
37. J. P. Lian, S. Stone, Y. Jiang, P. Lyons, S. Ferro-Novick, *Nature* **372**, 698 (1994).
38. V. V. Lupashin and M. G. Waters, *Science* **276**, 1255 (1997).
39. M. Kito *et al.*, *Biochem. Biophys. Res. Commun.* **220**, 653 (1996).
40. M. Sogaard *et al.*, *Cell* **78**, 937 (1994).
41. C. Dascher, R. Ossig, D. Gallwitz, H. D. Schmitt, *Mol. Cell. Biol.* **11**, 872 (1991).
42. The 42-kD recycling form of syntaxin5 (*65*) was principally recovered in the p115 complex.
43. T. Rowe, C. Dascher, S. Bannykh, H. Plutner, W. E. Balch, *Science* **279**, 696 (1998).
44. C. Dascher and W. E. Balch, *J. Biol. Chem.* **271**, 15866 (1996).
45. Dithiobis(sulfosuccinimidylproprionate) (DTSSP; 100 μM) cross-linker was added to microsomes before incubation (control) or to the COPII vesicle fraction from a 1-ml budding reaction (25 times the standard budding reaction volume) for 15 min on ice and quenched with 50 mM tris-HCl (pH 7.8). Membranes (25 μl) were solubilized with 25 μl of 2× radioimmunoprecipitation assay (RIPA) buffer for 10 min on ice. Insoluble material was removed by centrifugation at 16,000*g* for 10 min. Supernatants were diluted 10-fold with RIPA buffer without SDS (final concentration of SDS was 0.1%) containing 2×10^7 M500 Dynabeads (Dynal, New York) coupled to p115 mAb 3A10. Immunoprecipitation was carried out for 2 hours at 4°C with rotation. Beads were washed four times for 5 min each with RIPA buffer without SDS, and bound proteins were eluted by boiling in SDS sample buffer supplemented with 10 mM DTT for 5 min. Amounts of SNAREs and SNARE-binding proteins recovered in the p115 complex on COPII vesicles (Fig. 4A, lane b) were determined by densitometry of immunoblots. Recovery was expressed as a percentage of the amount of specific protein recovered in the HSP of the normal in vitro incubation

minus the background levels observed in the HSP in the control (Sar1-GDP–containing) incubation that prevents COPII vesicle formation. In the microsome control, the level of p115-SNARE associations was less than 0.1%.
46. C. M. Carr, E. Grote, M. Munson, F. M. Hughson, P. J. Novick, *J. Cell Biol.* **146**, 333 (1999).
47. C. Ungermann, B. J. Nichols, H. R. Pelham, W. Wickner, *J. Cell Biol.* **140**, 61 (1998).
48. E. Grote and P. J. Novick, *Mol. Biol. Cell* **10**, 4149 (1999).
49. P. Uetz *et al.*, *Nature* **403**, 623 (2000).
50. GST-SNARE proteins were expressed in bacteria and purified on glutathione-Sepharose beads using standard methods. Immobilized GST-SNARE protein (0.5 μM) was incubated with rat liver cytosol (20 mg) or purified recombinant p115 (0.5 μM) in 1 ml of NS buffer containing 1% BSA for 2 hours at 4°C with rotation. Beads were briefly spun (3000 rpm for 10 s) and sequentially washed three times with NS buffer and three times with NS buffer supplemented with 150 mM NaCl. Bound proteins were eluted three times in 50 μl of 50 mM tris-HCl (pH 8.5), 50 mM reduced glutathione, 150 mM NaCl, and 0.1% Triton X-100 for 15 min at 4°C with intermittent mixing, and elutes were pooled. Proteins were precipitated by MeOH/CH_3Cl and separated by SDS–polyacrylamide gel electrophoresis (PAGE) followed by immunoblotting using p115 mAb 13F12.
51. V. Rybin *et al.*, *Nature* **383**, 266 (1996).
52. K. G. Hardwick and H. R. Pelham, *J. Cell Biol.* **119**, 513 (1992).
53. A. P. Newman, M. E. Groesch, S. Ferro-Novick, *EMBO J.* **11**, 3609 (1992).
54. A. Spang and R. Schekman, *J. Cell Biol.* **143**, 589 (1998).
55. M. F. Rexach, M. Latterich, R. W. Schekman, *J. Cell Biol.* **126**, 1133 (1994).
56. A. Mayer and W. Wickner, *J. Cell Biol.* **136**, 307 (1997).
57. M. D. Turner, H. Plutner, W. E. Balch, *J. Biol. Chem.* **272**, 13479 (1997).
58. A. Price, D. Seals, W. Wickner, C. Ungermann, *J. Cell Biol.* **148**, 1231 (2000).
59. X. Cao and C. Barlowe, *J. Cell Biol.* **149**, 55 (2000).
60. G. G. Tall, H. Hama, D. B. DeWald, B. F. Horazdovsky, *Mol. Biol. Cell* **10**, 1873 (1999).
61. C. G. Burd, M. Peterson, C. R. Cowles, S. D. Emr, *Mol. Biol. Cell* **8**, 1089 (1997).
62. M. R. Peterson, C. G. Burd, S. D. Emr, *Curr. Biol.* **9**, 159 (1999).
63. M. G. Waters, D. O. Clary, J. E. Rothman, *J. Cell Biol.* **118**, 1015 (1992).
64. D. M. Walter, K. S. Paul, M. G. Waters, *J. Biol. Chem.* **273**, 29565 (1998).
65. N. Hui *et al.*, *Mol. Biol. Cell* **8**, 1777 (1997).
66. T. E. Kreis, *EMBO J.* **5**, 931 (1986).
67. H. Plutner, H. W. Davidson, J. Saraste, W. E. Balch, *J. Cell Biol.* **119**, 1097 (1992).
68. D. S. Nelson *et al.*, *J. Cell Biol.* **143**, 319 (1998).
69. We thank G. Waters for p115 cDNA and p115 mAbs; G. Warren for p97 and p47 antibodies; R. Scheller for rbet1, membrin, and sec22 cDNAs; H. Plutner for excellent technical assistance; and P. Tan for help during the initial phase of this work. Supported by NIH grants GM 33301 and GM42336 and National Cancer Institute grant CA58689 (W.E.B.), a NIH National Research Service Award (B.D.M.), and a Wellcome Trust International Traveling Fellowship (B.B.A.).

20 March 2000; accepted 22 May 2000

One Sequence, Two Ribozymes: Implications for the Emergence of New Ribozyme Folds

Erik A. Schultes and David P. Bartel*

We describe a single RNA sequence that can assume either of two ribozyme folds and catalyze the two respective reactions. The two ribozyme folds share no evolutionary history and are completely different, with no base pairs (and probably no hydrogen bonds) in common. Minor variants of this sequence are highly active for one or the other reaction, and can be accessed from prototype ribozymes through a series of neutral mutations. Thus, in the course of evolution, new RNA folds could arise from preexisting folds, without the need to carry inactive intermediate sequences. This raises the possibility that biological RNAs having no structural or functional similarity might share a common ancestry. Furthermore, functional and structural divergence might, in some cases, precede rather than follow gene duplication.

Related protein or RNA sequences with the same folded conformation can often perform very different biochemical functions, indicating that new biochemical functions can arise from preexisting folds. But what evolutionary mechanisms give rise to sequences with new macromolecular folds? When considering the origin of new folds, it is useful to picture, among all sequence possibilities, the distribution of sequences with a particular fold and function. This distribution can range very far in sequence space (*1*). For example, only seven nucleotides are strictly conserved among the group I self-splicing introns, yet secondary (and presumably tertiary) structure within the core of the ribozyme is preserved (*2*). Because these disparate isolates have the same fold and function, it is thought that they descended from a common ancestor through a series of mutational variants that were each functional. Hence, sequence heterogeneity among divergent isolates implies the existence of paths through sequence space that have allowed neutral drift from the ancestral sequence to each isolate. The set of all possible neutral paths composes a "neutral network," connecting in sequence space those widely dispersed sequences sharing a particular fold and activity, such that any sequence on the network can potentially access very distant sequences by neutral mutations (*3*–*5*).

Theoretical analyses using algorithms for predicting RNA secondary structure have suggested that different neutral networks are interwoven and can approach each other very closely (*3*, *5*–*8*). Of particular interest is whether ribozyme neutral networks approach each other so closely that they intersect. If so, a single sequence would be capable of folding into two different conformations, would have two different catalytic activities, and could access by neutral drift every sequence on both networks. With intersecting networks, RNAs with novel structures and activities could arise from previously existing ribozymes, without the need to carry nonfunctional sequences as evolutionary intermediates. Here, we explore the proximity of neutral networks experimentally, at the level of RNA function. We describe a close apposition of the neutral networks for the hepatitis delta virus (HDV) self-cleaving ribozyme and the class III self-ligating ribozyme.

In choosing the two ribozymes for this investigation, an important criterion was that they share no evolutionary history that might confound the evolutionary interpretations of our results. Choosing at least one artificial ribozyme ensured independent evolutionary histories. The class III ligase is a synthetic ribozyme isolated previously from a pool of random RNA sequences (*9*). It joins an oligonucleotide substrate to its 5′ terminus. The prototype ligase sequence (Fig. 1A) is a shortened version of the most active class III variant isolated after 10 cycles of in vitro selection and evolution. This minimal construct retains the activity of the full-length isolate (*10*). The HDV ribozyme carries out the site-specific self-cleavage reactions needed during the life cycle of HDV, a satellite virus of hepatitis B with a circular, single-stranded RNA genome (*11*). The prototype HDV construct for our study (Fig. 1B) is a shortened version of the antigenomic HDV ribozyme (*12*), which undergoes self-cleavage at a rate similar to that reported for other antigenomic constructs (*13*, *14*).

The prototype class III and HDV ribozymes have no more than the 25% sequence identity expected by chance and no fortuitous structural similarities that might favor an intersection of their two neutral networks. Nevertheless, sequences can be designed that simultaneously satisfy the base-pairing requirements

Whitehead Institute for Biomedical Research and Department of Biology, Massachusetts Institute of Technology, 9 Cambridge Center, Cambridge, MA 02142, USA.

*To whom correspondence should be addressed. E-mail: dbartel@wi.mit.edu